Indian Journal of Pure & Applied Physics
Vol. 53, June 2015, pp. 371-375

Enhancement of asymmetric acoustic transmission based on a plate with periodic stepped resonators

Hongbo Zhang, Jiujiu Chen* & Xu Han

State Key Laboratory of Advanced Design and Manufacturing for Vehicle Body,
College of Mechanical and Vehicle Engineering, Hunan University, Changsha, 410082, People's Republic of China

*E-mail: chen99nju@gmail.com

Received 13 October 2014; revised 2 February 2015; accepted 9 April 2015

A steel plate with periodic stepped resonators immersed in water has been presented to enhance the asymmetric acoustic transmission (AAT) in the present paper. It results from the re-emitted waves at resonance by the cap which would act as a secondary source. By changing the geometrical parameters of the stepped resonator, the AAT phenomenon can be tuned easily. The proposed acoustic system may have potential impact on underwater acoustic and medical ultrasonic devices in sub-wavelength region.

Keywords: Asymmetric acoustic transmission, Periodic stepped resonators, Secondary source

1 Introduction

The asymmetric acoustic transmission has become a hot research topic in recent years due to the extensive applications in a variety of important fields, such as acoustic one-way mirrors, acoustic rectifiers and related medical devices[1-7]. It can be realized by breaking the time-reversal symmetry or the spatial inversion symmetry. Liang *et al*[8,9]. have first realized the AAT by coupling a superlattice with a strongly nonlinear medium. The AAT owes to the creation of the second harmonic wave. Considering the low efficiency, the difficulty in fabrication and the frequency shift of the transmitted waves for the broken time-reversal symmetry case, much attention has been paid to breaking the spatial inversion symmetry. Shirota *et al*[10]. have proposed an AAT structure comprising of an array of triangular holes drilled in an elastically isotropic material. The AAT phenomenon appears above a threshold frequency due to the Bragg diffraction owing to the periodic structures. Li *et al*[11]. have demonstrated both theoretically and experimentally that unidirectional acoustic transmission can be achieved through a simple structure consisting of only a uniform stiff plate and periodic rectangular gratings, which is attributed to one-side pattern reconstruction of acoustic plane waves induced by the periodic gratings. However, a resonant cavity should be reserved between the gratings and the uniform plate. Soon after, Jia *et al*[12]. have proposed a system consisting of a steel plate patterned with periodic ridges on one side immersed in water to get acoustic unidirectional transmission by asymmetrically exciting the Lamb modes in the single-sided patterned steel plate. The frequency and efficiency of the AAT can be tuned by changing the period; however, the shifting ranges of the frequency and efficiency of the AAT are relatively limited with the change of the period.

In the present paper, it is demonstrated that enhancement of AAT can be realized in the sub-wavelength region for a steel plate with periodic stepped resonators. As comparison, a uniform steel plate with periodic rectangular gratings on one side is used. The spatial intensity distributions of the acoustic pressure field in the water and the total displacement distribution of the vibration in the uniform plate and stepped resonators are analyzed. The locally resonant （LR） element plays the crucial role. Moreover, the effect of the geometrical parameters of the stepped resonators on the AAT is studied.

2 Model and Method

A unit cell is schematically shown in Fig. 1, which consists of a uniform steel plate (thickness t=1 mm) patterned with periodic steel stepped resonators (period p=4 mm) on one side, immersed in water. The stepped resonator is comprised of a rib plate (width w_1=1 mm and thickness t_1=1 mm) and a cap plate (width w_2=2 mm and thickness t_2=1 mm). The rib

plate connects the cap plate and the uniform plate. The material parameters are adopted as follows: the density ρ=7890 kg/m^3, the longitudinal wave velocity c_l=5780 m/s, and the transversal wave velocity c_t=3100 m/s for steel structure; ρ=1000 kg/m^3, and c_w=1498 m/s for water. The normal incidence of acoustic waves from the structured side is defined as positive incidence (PI), while that from the smooth side is defined as negative incidence (NI). The finite element method (FEM) is employed for numerical simulations. In the numerical simulations, one primitive cell is considered and the periodic boundary conditions are imposed on the z direction and the perfectly matched layer is imposed on the output side[13,14].

In order to test the acoustic transmission spectra calculated by FEM, the finite difference time domain (FDTD) method is also presented[15-17]. The governing equations of acoustic motion can be written conveniently in a set of canonical, first order equations as:

$$\frac{\partial v_x}{\partial t}=\frac{1}{\rho}\left(\frac{\partial \sigma_{xx}}{\partial x}+\frac{\partial \sigma_{xy}}{\partial y}\right) \quad \ldots(1)$$

$$\frac{\partial v_y}{\partial t}=\frac{1}{\rho}\left(\frac{\partial \sigma_{xy}}{\partial x}+\frac{\partial \sigma_{yy}}{\partial y}\right) \quad \ldots(2)$$

$$\sigma_{xx}=(\lambda+2\mu)\frac{\partial v_x}{\partial x}+\lambda\frac{\partial v_y}{\partial y} \quad \ldots(3)$$

$$\sigma_{yy}=(\lambda+2\mu)\frac{\partial v_y}{\partial y}+\lambda\frac{\partial v_x}{\partial x} \quad \ldots(4)$$

$$\sigma_{xy}=\mu\left(\frac{\partial v_x}{\partial y}+\frac{\partial v_y}{\partial x}\right) \quad \ldots(5)$$

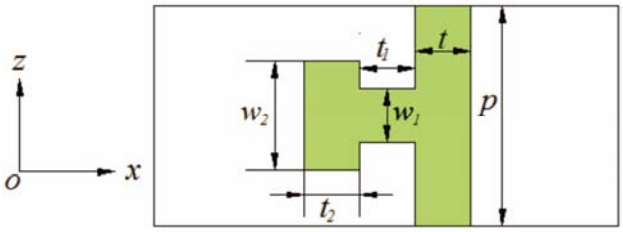

Fig. 1 — Schematic diagram of the proposed structure, which consists of a uniform steel plate patterned with periodic steel stepped resonators on one side, immersed in water. The stepped resonator consists of a rib plate and a cap plate

where v and σ are the velocity vector and stress tensor, λ and μ are the Lamé coefficients of the material and ρ is the mass density. Due to the periodicity of the composite ρ, λ and μ are discontinuous functions of the positions, which can be connected through the relations $\mu=\rho c_t^2$ and $\lambda=\rho c_l^2-2\mu$, where c_t and c_l are separately the transverse and longitudinal components of the wave speed. Fluid is treated here as a solid with zero transverse speed of sound.

3 Results and Discussion

To test our methods, the transmission spectra of the proposed structure for PI are shown in Fig. 2. The acoustic transmission coefficients by FE method are found to be in good agreement with those in FDTD method (Fig. 2). Then the power transmission spectra through the proposed structure (stepped case) for PI and NI are shown in Fig. 3. For comparison, the power transmission spectra of a steel plate with rectangular gratings (the cap plate is removed) on one side (reference case) for PI and NI are also shown in Fig. 3. The proposed structure for PI has high transmission efficiency, but the transmission of the proposed structure for NI and the reference case for PI and NI are rather low. It is obviously observed that a remarkable transmission peak of the proposed structure for PI is located at 680 kHz with a large power transmission 0.84. In other words, the proposed structure has enhanced AAT performance while the reference case has almost no transmission difference.

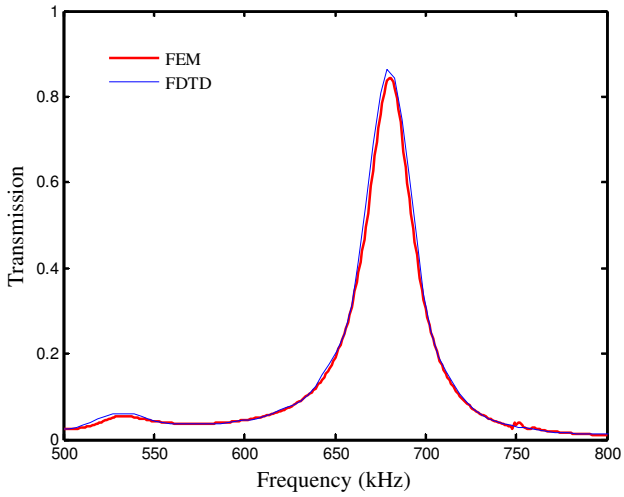

Fig. 2 — Transmission spectra of the proposed structure for PI are calculated by FEM method (red line) and FDTD method (blue line)

It should be noted that the frequency of the transmission peak for PI matches neither the Wood's anomaly nor the Fabry-Perot resonance because the wavelength of the peak λ_p=1.74 mm is smaller than the period.

In order to understand the physical mechanism behind the AAT, the spatial intensity of acoustic fields in water and the total displacement distributions in steel structure at 680 kHz are shown in Fig. 4. The vibrations in the cap plate and the uniform plate are strong in Fig. 4(a). This case can transmit most energy of the incident acoustic waves through the steel structure. The vibration configuration in the structured plate demonstrates that the excited mode is a typical anti-symmetric Lamb mode. So it is clear that the anti-symmetric Lamb mode plays an important role. On the contrary, the case of Fig. 4(b) can transmit a little energy through the steel structure, because most of acoustic waves are reflected by the smooth surface. The reference cases in Figs 4(c) and (d) block most energy of the incident acoustic waves and can transmit negligible energy through the steel plate. As shown in Fig. 4, the vibration in the stepped case is stronger than that of the reference case for PI and NI. In order to find the mechanism, the phase of the transmitted waves has been analyzed. If the phase of the transmitted waves in the stepped case is different from that of the reference case, the transmitted waves are re-emitted by the cap which would act as a secondary source. Then, the phase of the pressure of the middle point in the receiver line for all considered cases has been calculated. The phase in the reference case is about −39.1° (−23.8°) for PI (NI), while that of the stepped case is 83.8° (−83.3°). This elucidates that the phase of the transmitted waves is changed by the cap. From the above analysis, it is concluded that the asymmetric acoustic propagation phenomenon results from the re-emitted waves at resonance by the cap which would act as a secondary source.

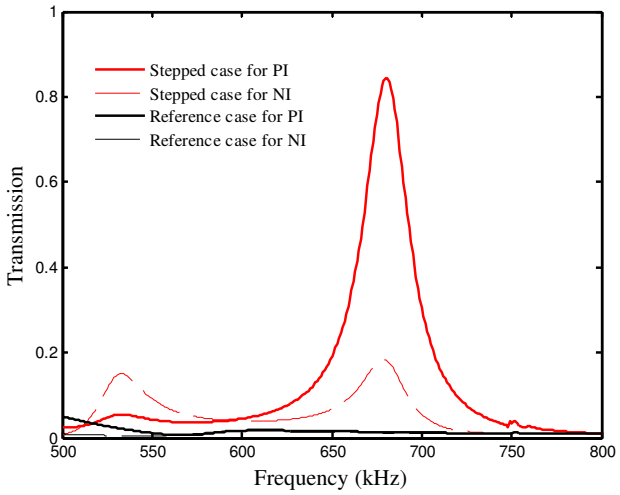

Fig. 3—Power transmission spectra through the proposed structure (red line for PI, red dashed line for NI) and the reference case for PI and NI (black line for PI, black dashed line for NI)

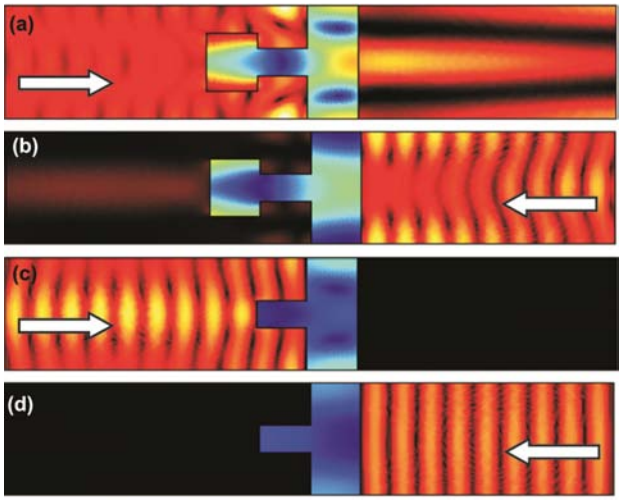

Fig. 4 — Spatial intensity of acoustic fields in water and the total displacement distributions in steel structure at 680 kHz: (a) stepped case for PI, (b) stepped case for NI, (c) reference case for PI, (d) reference case for NI. The arrows in the figures indicate the directions of incident waves

At last, the effect of the geometrical parameters of the stepped resonator on the AAT has been studied. The value of the transmission peak for PI (NI) is defined as t_p (t_n). The AAT is evaluated by the transmission difference value t_d=t_p−t_n. Figure 5 shows the transmissions as a function of the geometrical parameters w_1, t_1, w_2 and t_2, respectively. It can be observed that the AAT phenomena are dependent on these factors. Figure 5(a) shows the evolution of the transmission as a function of w_1 with p=4 mm, t_1=1 mm, w_2=2 mm and t_2=1 mm. As shown in Fig. 5(a), three points should be noted. First, the locations of the transmission peaks for PI and NI are pushed to high frequency region with the increase of w_1. Second, the transmission peaks for PI and NI appear at the same frequency. Third, the increase of w_1 has different effect on the values of the transmission peaks for PI and NI. With the increase of w_1, the value of the transmission peak first increases and then decreases for PI (t_p=7.33, 0.805, 0.844, 0.839), while for the NI case (t_n=0.135, 0.157, 0.182, 0.208), the value of the

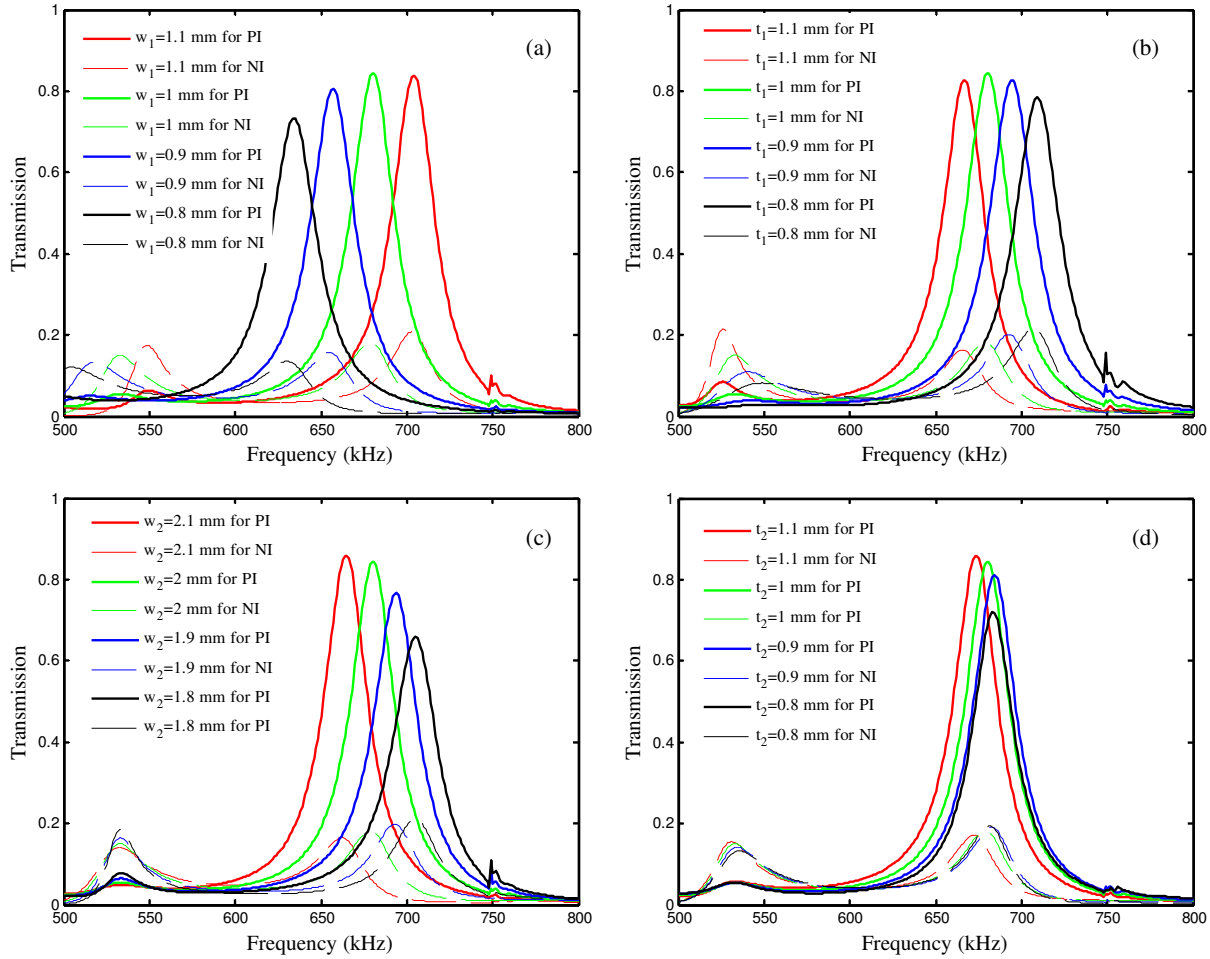

Fig. 5 — Frequency of the AAT as a function of the geometrical parameters. The transmission varied with the changes of the width of the rib plate w_1 (a), the thickness of the rib plate t_1 (b), the width of the cap plate w_2 (c), and the thickness of the cap plate t_2 (d)

transmission peak is monotonously increased. So the AAT (t_1=0.598, 0.648, 0.662, 0.631) is first enhanced and then weakened. Figure 5(b) shows the evolution of the transmission as a function of t_1 with p=4 mm, w_1=1 mm, w_2=2 mm and t_2=1 mm. An interesting phenomenon can be observed from Fig. 5(b) that the increase of t_1 leads to smaller value of the transmission peak for NI (t_n=0.217, 0.200, 0.182, 0.163), while the increase of t_1 leads to larger value of the transmission peak for PI (t_p=0.784, 0.827, 0.844, 0.827) and then the value of the transmission peak decreases. This indicates that the AAT (t_d=0.567, 0.627, 0.662, 0.664) can be improved greatly by changing t_1. In addition, the transmission peaks also appear at the same frequency for PI and NI. The locations of the transmission peaks are pressed into the low frequency region. Figure 5(c) shows the evolution of the transmission as a function of w_2 with p=4 mm, w_1=1 mm, t_1=1 mm and t_2=1 mm. Figure 5(c) shows that the locations of the transmission peaks for PI and NI are pushed to low frequency region with the increase of w_2. The value of the transmission peak for PI (t_p=0.658, 0.766, 0.844, 0.859) is increased with the increase of w_2. On the contrary, the value of the transmission peak for NI (t_n=0.212, 0.198, 0.183, 0.165) is decreased. In other words, the AAT (t_d=0.446, 0.568, 0.661, 0.694) is obviously enhanced by changing w_2. Figure 5(d) shows the evolution of the transmission as a function of t_2 with p=4 mm, w_1=1 mm, t_1=1 mm and w_2=1 mm. Figure 5(d) shows that the locations of the transmission peaks for PI and NI are slightly pushed to low frequency region with the increase of t_2. The value of the transmission peak for PI (t_p=0.719, 0.811, 0.844, 0.859) is increased with the increase of t_2. On the contrary, the value of the transmission peak for NI

(t_n=0.194, 0.192, 0.183, 0.172) is decreased. The AAT (t_d=0.525, 0.619, 0.661, 0.687) is also enhanced by the change of t_2. These results show that the dependence of the locations of the transmission peaks on w_1, t_1, w_2 and t_2 agrees with the results predicted by using the spring-mass model[13,18,19]. The AAT can be adjusted easily by changing w_1, t_1, w_2 and t_2, respectively.

4 Conclusions

In summary, a steel plate with periodic stepped resonators immersed in water has been studied by using FEM and FDTD methods. The results show that the AAT results from the re-emitted waves at resonance by the cap, would act as a secondary source. The AAT can be adjusted easily by changing the geometrical parameters of the resonator. Such kind of AAT could open possibilities in directional de-noise and signal detection in underwater.

Acknowledgement

The authors gratefully acknowledge financial support from National Science Foundation of China under Grant No.11374093, the Program of the State Key Laboratory of Advanced Design and Manufacturing for Vehicle Body No.71375006, the Hunan University Young Teacher Growth Scheme Funding and Hunan Provincial Innovation Foundation for Postgraduate.

References

1 Lepri S & G Casati, *Phys Rev Lett*, 106 (2011) 164101.
2 Li Y, Liang B, Gu Z M, Zou X Y & Cheng J C, *Appl Phys Lett*, 103 (2013) 053505.
3 Chen J J, Han X & Li G Y, *J Appl Phys*, 113 (2013) 184506.
4 Zhu X F, Zou X Y, B L & Cheng J C, *J Appl Phys*, 108 (2012) 124909.
5 He Z J, Peng S S, Ye Y T, Dai Z W, Qiu C Y, Ke M Z & Liu Z Y, *Appl Phys Lett*, 98 (2011) 083505.
6 Nishiguchi N, Tanaka Y & Murai T, *J Appl Phys*, 46 (2007) 1025.
7 Maznev A A, Every A G & Wright O B, *Wave Motion*, 50 (2013) 776.
8 Liang B, Yuan B & Cheng J C, *Phys Rev Lett*, 103 (2007) 104301 (2009).
9 Liang B, Guo X S, Tu J, Zhang D & Cheng J C, *Nature Mater*, 9 (2010) 989.
10 Krishnan R, Shirota S, Tanaka Y & Nishiguchi N, *Solid State Commun*, 144 (2007) 194.
11 Li Y, Tu J, Liang B, Guo X S, Zhang D & Cheng J C, *J Appl Phys*, 112 (2012) 064504.
12 Jia H, Ke M Z, Li C H, Qiu C Y & Liu Z Y, *Appl Phys Lett*, 102 (2013) 153508.
13 Li Y, Liang B, Zou X & Cheng J, *Chin Phys Lett*, 29 (2012) 114301.
14 Zhang H B, Chen J J & Han X, *Phys Lett A*, 377 (2013) 2226.
15 Su X X & Wang Y S, *Physica B*, 405 (2010) 3645.
16 Lambin Ph & Khelif A, *Phys Rev E*, 63 (2001) 066605.
17 Cai F, Meng L, Jiang C, Pan Y & H Zheng, *J Acoust Soc Am*, 128 (2010) 4.
18 Goffaux C, Sánchez-Dehesa J, Yeyati A, Lambin P, Khelif A, Vasseur J & Djafari-Rouhani B, *Phys Rev Lett*, 88 (2002) 225502.
19 Oudich M, Li Y, Assouar B M & Hou Z L, *New J Phys*, 12 (2010) 083049.